

Interaction of radio jets with clouds in the ambient medium: Numerical simulations

Solai Jeyakumar*

Departamento de Astronomía, Universidad de Guanajuato, AP 144, Guanajuato CP 36000, Mexico.

The dates of receipt and acceptance should be inserted later

Key words methods: numerical - ISM: clouds - galaxies: active - galaxies: jets

Hydrodynamical simulations of jets interacting with clouds moving in the ambient medium of the host galaxy are presented. Clouds with sizes of the order of the jet diameter and smaller, crossing the path of the jet with different speeds are considered. In the case of slow moving clouds the jet is stopped over the brief period of time taken by the cloud to cross the jet. The jet maintains its general morphology in the case of fast moving clouds. Erosion of the clouds leads to redistribution of cloud material to large distances. Such interaction may explain the large outflow velocities observed from pc to kpc scales in the compact radio sources.

© WILEY-VCH Verlag GmbH & Co. KGaA, Weinheim

1 Introduction

The Gigahertz Peaked Spectrum (GPS) and the Compact Steep Spectrum (CSS) sources (cf. O’Dea 1998, for a review) are young radio sources evolving in the Inter Stellar Medium (ISM) of the galaxies hosting them. The radio morphology of these sources show evidence of interaction of the radio jets with inhomogeneities in the ISM. (Jeyakumar et al. 2005; Saikia et al. 1995). Several observations of the line emitting gas in the optical and radio wavelengths, show further evidence for such interactions. Observations of the gas at large scales reveal that the line emission from the narrow line regions (NLRs) and the cold neutral HI clouds show complex velocity profiles and outflows (de Vries et al. 1999; Emonts et al. 2005; Labiano 2008; Labiano et al. 2005; Morganti, Tadhunter, & Oosterloo 2005; O’Dea et al. 2003). In addition, outflows have been observed in the broad components. These observations reveal outflows of line emitting gas with velocities ranging from a few 100 km/s to more than 1000 km/s, from pc to kpc scales, both in the ionised and the neutral components (cf. Holt, Tadhunter & Morganti 2003, 2008; Morganti et al. 2005). Modelling of lines of high ionisation state (Gupta, Srikanth & Saikia 2005), as well as several narrow lines (Labiano et al. 2005), suggest that there is a contribution by shocks to the ionisation of the gas. All these observations suggest that interaction of jets with clouds in the ISM could play a role in the ionisation and outflow of the gas.

Numerical simulations have been successfully used to study the effects of propagation of radio jets through a variety of ambient atmospheres (cf. Carvalho & O’Dea 2002; Hooda & Wiita 1996; Jeyakumar et al. 2005; Krause 2005; Wiita & Norman 1992). Such studies can be used to under-

stand the relation between the outflow and the ionisation of the gas. In fact, several numerical studies have been attempted to study the interaction of the jets with clouds in the ambient medium (Choi, Wiita, & Ryu 2007; Fragile et al. 2004; Higgins, O’Brien, & Dunlop 1999; Wang, Wiita, & Hooda 2000; Xu & Stone 1995). All these studies focused on the evolution of the individual clouds and the effect of the clouds on the dynamics and morphology of the radio source. The clouds in these studies are large and massive resembling diffuse neutral clouds in the ISM of the Galaxy. A few simulations of jet propagation in a clumpy medium have been carried out where a few of them also considered parameters similar to that of the CSS/GPS sources, but with a lower jet kinetic power (Saxton et al. 2005; Steffen et al. 1997; Sutherland & Bicknell 2007).

In all of these simulations, the jet collides with a static cloud or a dense clumpy structure in the ambient medium. However, a more realistic scenario is dense small clouds such as those expected in the NLR and BLRs that move into to the path of the jet/lobe. Such a scenario is more probable for the young radio sources where the radio jet has not cleared the natal cocoon of material of the ISM yet. So, here simulations of clouds moving into the jet are attempted.

2 Jet cloud interaction

The line emitting regions of the ISM are expected to be clumpy and turbulent. It can be approximated as a hot tenuous inter-clump medium with spherical clumps embedded in it. There are two ranges of densities and scale sizes of the clumps in the ISM that show outflows: (a) the NLRs and dense large neutral clouds ($n \sim 10^{2-5} \text{ cm}^{-3}$) at kpc scales and, (b) BLRs with very high densities ($n \sim 10^{11} \text{ cm}^{-3}$) but at sub-pc scales (cf. Ferland et al. 1992; Laor et al. 1997; Sulentic, Marziani, & Dultzin-Hacyan 2000; Xu et al. 2007).

* Corresponding author: e-mail: sjk@astro.ugto.mx

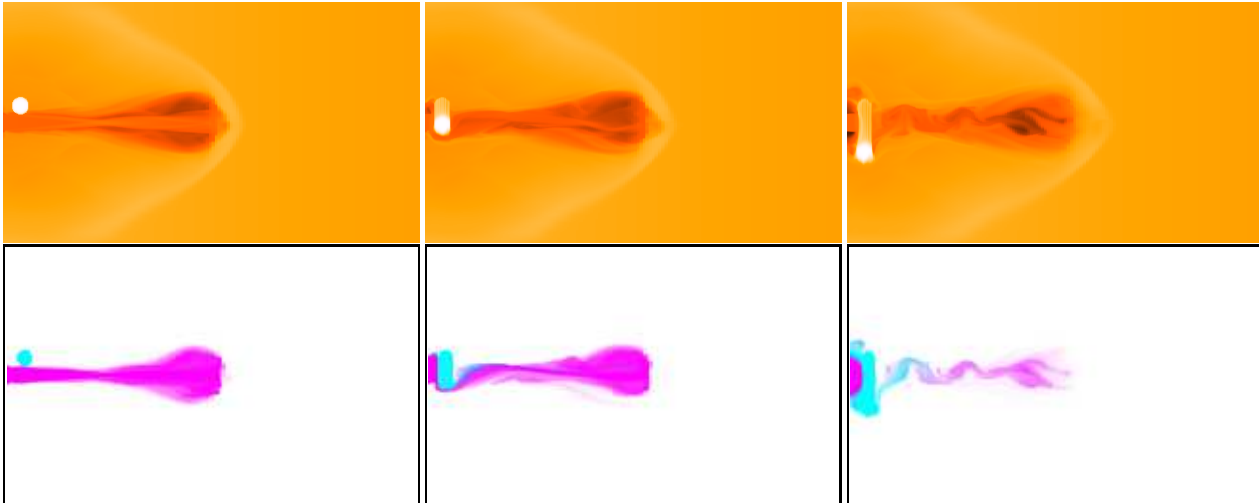


Fig. 1 Snapshots of the logarithm of density (top) and the Lagrangian tracers of the cloud and jet material (bottom) of the run F1 are shown. The images from left to right correspond to 1.0, 1.04 and 1.12 problem time units. Cyan color (light gray) represents the cloud material and magenta (dark gray) represents the jet material. The radius of the jet and the size of the cloud are scaled to 100 pc. In this unit the total extent of the visible jet is about 3 kpc (left panel).

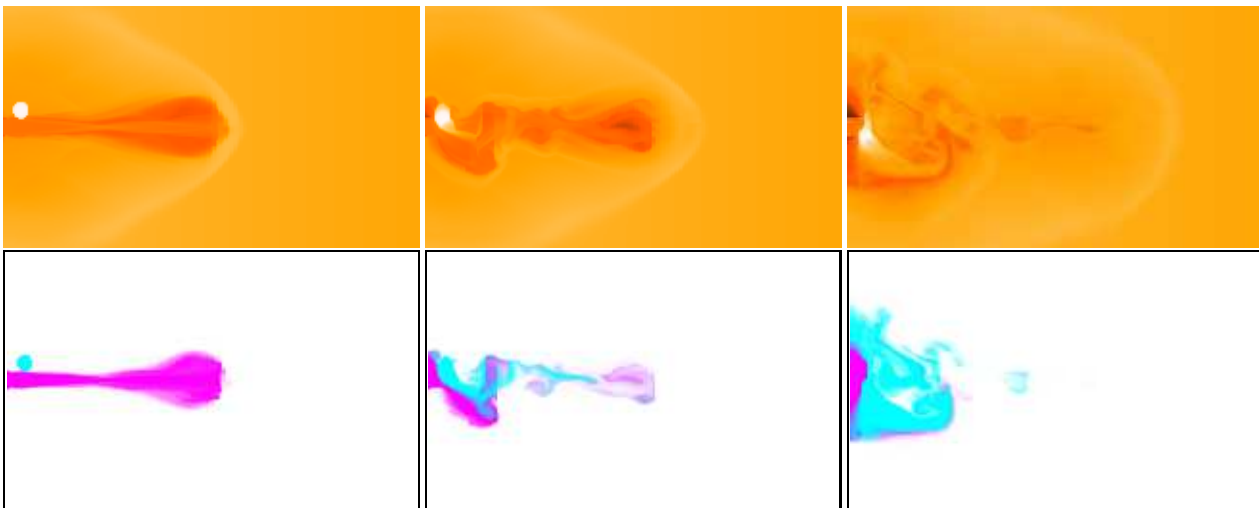


Fig. 2 Same as Fig 1, but for the run S1 (slow cloud). The snapshot times are 1.0, 1.18 and 1.65 problem time units from left to right. The radius of the jet is scaled to 100 pc and the size of the cloud is 100 pc. In this unit the total extent of the visible jet is about 3 kpc (left panel).

To simulate a cloud with a typical density of BLR, a grid resolution of milli parsec is required. For the purpose of studying the overall dynamics involved in the interaction of the jet with a moving cloud, small dense clouds at two different velocities are considered. The density of the clouds considered here is comparable to that of the NLRs. The sizes of the clouds are chosen such that at least 10 zones span the cloud diameter. Because of this constraint the clouds are very massive. A smaller cloud spanning only 5 zones are also considered to reduce the mass of the cloud.

2.1 Numerical setup

Hydro-dynamical simulations in 3D were carried out using the ZEUSMP-V2.0 code, making use of the parallel fea-

ture that has become available with this code (Clarke 1996; Hayes et al. 2006; Stone & Norman 1992a,b). The jet problem was initialised based on the previous jet launching code (cf. Jeyakumar et al. 2005). For the simulations presented here a cluster of 20 processing cores were used. These simulations were run on a Cartesian grid with $180 \times 126 \times 22$ active zones spanning $50 R_j$ in the jet propagation direction, x , and $\pm 15 R_j$ in the cloud propagation direction, y , and $\pm 1.1 R_j$ in the z direction, where R_j is the radius of the jet. This choice allows us to consider a better resolution in two directions at the cost of a smaller physical extension in the third direction, although the resolution is the same. In the y direction, 80 uniform zones were used to span the inner $8 R_j$ region, while the rest of the zones were loga-

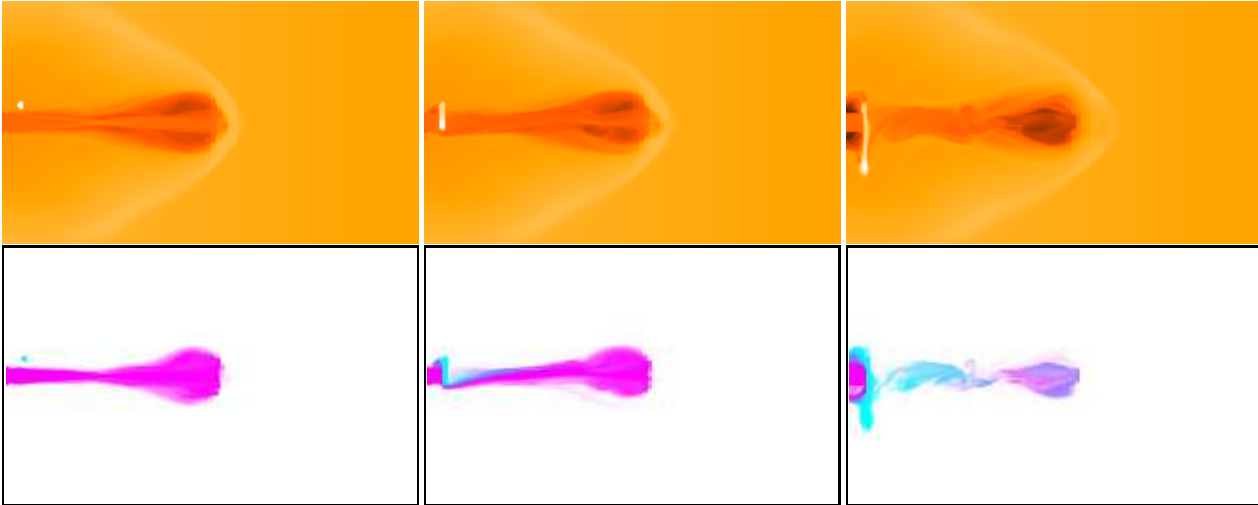


Fig. 3 Same as Fig 1, but for the run F2. The radius of the jet is scaled to 100 pc and the size of the cloud is 50 pc.

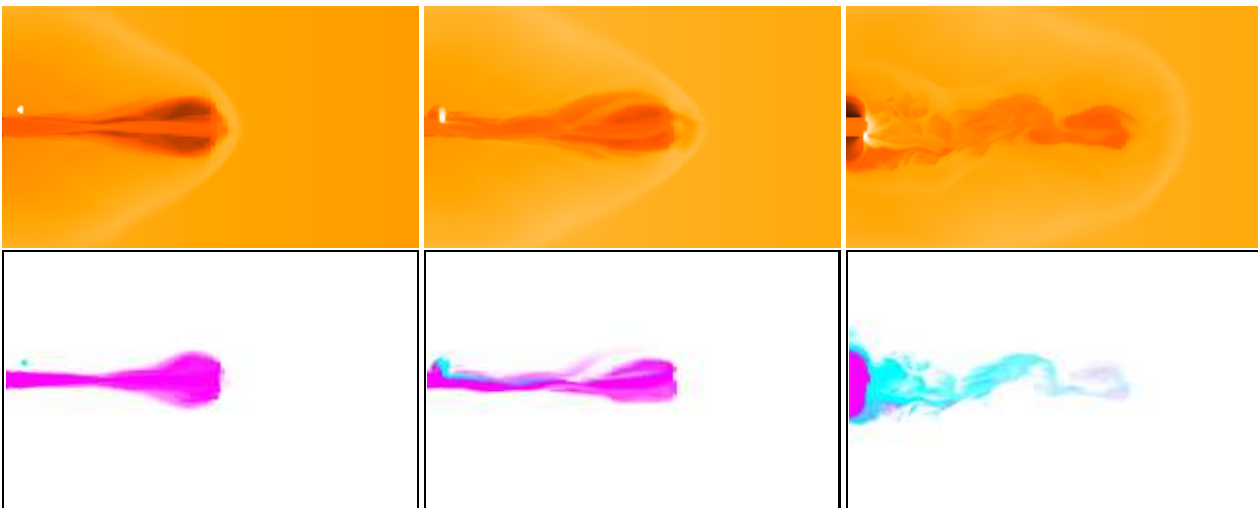


Fig. 4 Same as Fig 2, but for the run S2. The radius of the jet is scaled to 100 pc and the size of the cloud is 50 pc.

arithmically scaled. In the z direction all zones were uniformly spaced. In the x -direction logarithmic scaling was used. This enables us to track the propagation of the cloud with a reasonable resolution. Outflow boundary conditions were used everywhere except at the jet inlet, where inflow boundary condition was used.

The unit of length in this problem is the radius of the jet, R_j . The unit of time is given by the sound speed of the ambient medium, which was set to 1.0. The important parameters of the jet are the intrinsic Mach number, M_j , and the density, η , with respect to the ambient medium density. The initially pressure matched jet is assumed to be conical with a half opening angle of Ω . The ambient density is given as, $n_a(r) = n_0 / (1 + (r/a)^2)^\delta$, where a is the core radius, δ is the power law index of the density profile and r is the distance from the nucleus of the source.

The cloud is characterised by the central density, n_c , size, R_c , and a velocity with respect to the sound speed of the ambient medium, V_c . The density of the cloud is tapered

as $n_a(r) + (n_c - n_a(r)) \tanh((R_c - R) / (0.3 R_c))$, to avoid numerical artifacts (cf. Choi et al. 2007), where R is the distance from the centre of the cloud. The temperature of the cloud is varied in such a way that the pressure inside follows the pressure of the undisturbed ambient medium, although the cloud is introduced inside the region affected by the bow shock of the jet, leading to a small but negligible pressure difference between the cloud and the disturbed ambient medium. In addition, Lagrangian tracer variables are used to track the jet and the cloud materials using the multi-species advection scheme available with ZEUSMP V2.0 (see Hayes et al. (2006), for more details). These variables are set as 1.0 at the corresponding grid locations at the initial times.

The numerical parameters used in these simulations are, $M_j = 26$, $\eta = 0.001$, $a = 20 R_j$, $n_0 = 1.0$, $\delta = 0.75$ and $\Omega = 0.02$. After the jet has propagated to about $30 R_j$, the cloud is introduced at $x=2 R_j$, $y=2 R_j$ and $z=0$. The numerical runs F1 and F2 (called fast cloud) with an R_c of 1.0 and $0.5 R_j$ respectively are calculated with a velocity V_c

of 50. The numerical runs S1 and S2 (called slow cloud) are calculated with the same parameters but with a V_c of 5.

These simulations are scaled as follows: for a jet radius of 100 pc, and temperature of the ambient medium of 2×10^6 K, the time unit is 0.43 Myr and the jet power is 2×10^{45} erg/s. For these parameters the velocities of the fast and slow clouds are 10^4 and 10^3 km/s and the core radius of the density profile of the ambient medium is 2 kpc. The central density of the cloud is 10^3 cm $^{-3}$.

3 Results and Discussion

Color images of the logarithm of the density as well as the Lagrangian tracers of the jet and the cloud are shown in Fig 1 to Fig 4. These figures show the morphology of the jet and the cloud at different times: (a) when the cloud is launched, (b) when the cloud is half-way through the jet and (c) when the cloud has just passed through the jet. During the initial interaction of the cloud with the jet, erosion of the cloud material is seen (see the centre panels of the figures). The eroded cloud material is carried to large distances. Apart from this, the cloud remains as a clump blocking the path of the jet. At later stages, distortion of the cloud can be seen and the cloud material is distributed to a distance of about half the length of the lobe. At later stages when most part of the cloud has passed through the jet, a clump of material can be identified as a cloud, but compressed in the direction of propagation of the jet.

The time taken by the slow, small cloud to travel a distance of a jet diameter is about 3×10^5 yr, while the larger cloud takes somewhat longer time to cross through the jet. The jet is stopped completely in the slow cloud runs and the morphology is similar to that seen in other simulations of static clouds. In the fast cloud simulations, the cloud velocity is 10 times faster, thus the interaction times are smaller. These simulations also show the general morphology seen in the slow cloud runs. However, the jet is not completely stopped in these runs and the radio source maintains its general morphology. Although the parameters of the jet and those of the clouds used here are somewhat different between the simulations of interaction of the jets with static clouds (e.g. Higgins et al. 1999; Wang et al. 2000), these results can be compared with that of the static cloud simulations. The main difference is the erosion of the cloud material at the initial stages. Since the clouds are very massive, the clouds do not gain any velocity in the x direction. However, the eroded material seen at large distances during the initial encounter accelerates to large distances and can be compared with the outflow. At later times (the right panels of the figures), back flowing cocoon also carries the material backwards. In such a scenario the emission lines can be very complex.

In young radio sources where the radio jets are still expanding within the natal cocoon of a clumpy ISM, such interactions are likely to occur. Once the jet has emerged out of the ISM clearing the cocoon of material on its way, such

incidences are less likely to occur. Observations also indicate such a scenario (Inskip et al. 2002). These simulations also suggest that the distorted radio morphology and outflow can be correlated.

Acknowledgements. The work presented here was supported by PROMEP/103-5/07/2462 grant. I thank the referee Chris O'Dea for very useful comments.

References

- Carvalho, J.C., O'Dea, C.P.: 2002, *ApJS* 141, 371
 Choi, E., Wiita, P.J., Ryu, D.: 2007, *ApJ* 655, 769
 Clarke, D.A.: 1996, *ApJ* 457, 291
 de Vries, W.H., O'Dea, C.P., Baum, S.A., Barthel, P.D.: 1999, *ApJ* 526, 27
 Emonts, B.H.C., Morganti, R., Tadhunter, C.N., Oosterloo, T.A., Holt, J., van der Hulst, J.M.: 2005, *MNRAS* 362, 931
 Ferland, G.J., Peterson, B.M., Horne, K., Welsh, W.F., Nahar, S.N.: 1992, *ApJ* 387, 95
 Fragile, P.C., Murray, S.D., Anninos, P., van Breugel, W.: 2004, *ApJ* 604, 74
 Gupta, N., Srianand, R., Saikia, D.J.: 2005, *MNRAS* 361, 451
 Hayes, J.C., Norman, M.L., Fiedler, R.A., Bordner, J.O., Li, P.S., Clark, S.E., Ud-Doula, A., Mac Low, M.-M.: 2006, *ApJS* 165, 188
 Higgins, S.W., O'Brien, T.J., Dunlop, J.S.: 1999, *MNRAS* 309, 273
 Holt, J., Tadhunter, C.N., Morganti, R.: 2003, *MNRAS* 342, 227
 Holt, J., Tadhunter, C.N., Morganti, R.: 2008, *MNRAS* 387, 639
 Hooda, J.S., Wiita, P.J.: 1996, *ApJ* 470, 211
 Inskip, K.J., Best, P.N., Rawlings, S., Longair, M.S., Cotter, G., Röttgering, H.J.A., Eales, S.: 2002, *MNRAS* 337, 1381
 Jeyakumar, S., Wiita, P.J., Saikia, D.J., Hooda, J.S.: 2005, *A&A* 432, 823
 Krause, M.: 2005, *A&A* 431, 45
 Labiano, A.: 2008, *A&A* 488, L59
 Labiano, A., O'Dea, C.P., Gelderman, R., et al.: 2005, *A&A* 436, 493
 Laor, A., Jannuzi, B.T., Green, R.F., Boroson, T.A.: 1997, *ApJ* 489, 656
 Morganti, R., Tadhunter, C.N., Oosterloo, T.A.: 2005, *A&A* 444, L9
 O'Dea, C.P.: 1998, *PASP* 110, 493
 O'Dea, C.P., de Vries, W.H., Koekemoer, A.M., et al.: 2003, *PASA* 20, 88
 Saikia, D.J., Jeyakumar, S., Wiita, P.J., Sanghera, H.S., Spencer, R.E.: 1995, *MNRAS* 276, 1215
 Saxton, C.J., Bicknell, G.V., Sutherland, R.S., Midgley, S.: 2005, *MNRAS* 359, 781
 Steffen, W., Gomez, J.L., Raga, A.C., Williams, R.J.R.: 1997, *ApJL* 491, L73
 Stone, J.M., Norman, M.L.: 1992a, *ApJS* 80, 753
 Stone, J.M., Norman, M.L.: 1992b, *ApJS* 80, 791
 Sulentic, J.W., Marziani, P., Dultzin-Hacyan, D.: 2000, *ARA&A* 38, 521
 Sutherland, R.S., Bicknell, G.V.: 2007, *ApJS* 173, 37
 Wang, Z., Wiita, P.J., Hooda, J.S.: 2000, *ApJ* 534, 201
 Wiita, P.J., Norman, M.L.: 1992, *ApJ* 385, 478
 Xu, D., Komossa, S., Zhou, H., Wang, T., Wei, J.: 2007, *ApJ* 670, 60
 Xu, J., Stone, J.M.: 1995, *ApJ* 454, 172